A Solution to Timing Mismatches between the In-Phase and Quadrature Branches of Millimeter-wave Transmitter and Receiver

Qi Zhan[(1)], *Student Member, IEEE,* Hlaing Minn[(1)], *Fellow, IEEE,*
Naofal Al-Dhahir[(1)], *Fellow, IEEE,* Huang Huang[(2)], *Member, IEEE*
[(1)] University of Texas at Dallas, Richardson, TX, USA.
[(2)] Huawei Technologies Co., Ltd., Shenzhen, China

***Abstract*—This paper investigates the effect of in-phase and quadrature timing mismatch (IQTM) on millimeter-wave system performance and reveals that the IQTM, which is commonly neglected in the literature, degrades system performance significantly. As a solution to this IQTM problem, this paper proposes novel pilot designs for transmit and receive IQTM estimation, and develops corresponding estimators. Simulation results show that our proposed pilot designs and estimators offer an efficient solution to the IQTM problem.**

***Index Terms*—IQ timing mismatch, Pilot designs, Estimation, RF distortions, Millimeter-wave**

I. Introduction

RF distortions are non-negligible for the emerging millimeter-wave systems [1]–[3]. The existing RF distortion estimation/compensation schemes usually focus on in-phase and quadrature amplitude and phase imbalance (IQI) [4]–[10], phase noise (PN) or PN plus carrier frequency offset (CFO) [11], PN plus IQI [12], [13]. Due to CMOS process variations and the very high sampling frequency used in the millimeter-wave regime, the difference in signal propagation and processing times of the circuits between the in-phase and quadrature parts of the signal could be significant relative to the sampling interval. This leads to a timing (delay) mismatch between the in-phase and quadrature paths, which we term in-phase and quadrature timing mismatch (IQTM), at both the transmitter (TX) and receiver (RX). To the best of our knowledge, there are only a couple of existing works [14] and [15] which are related to IQTMs. Reference [14] considered a 4x4 MIMO-OFDM system and proposed a method for estimation and compensation of IQTM. Reference [15] evaluated effects of IQTM on the system performance for an optical communication system, but no estimation and compensation schemes were proposed. Both [14] and [15] consider RX IQTM only, thus, they are not applicable to systems with TX IQTMs. Furthermore, other RF distortions such as PN and CFO were not included in their study, which limits the applicability of their methods/results.

Our main contributions in this paper are pilot designs for IQTM estimation and corresponding IQTM estimators for systems with several RF distortions such as PN, CFO, IQI, and IQTM at both TX and RX.

The rest of the paper is organized as follows. Section II presents signal model and Section III describes pilot designs for IQTM. Estimation and compensation of IQTM are described in Section IV. Performance evaluation results are discussed in Section V. Conclusions are provided in Section VI.

II. Signal Model with RF Distortions including DAC/ADC IQ Timing Mismatches

In this section, we develop the signal model under various RF distortions such as CFO, PN, IQI, sampling frequency offset (SFO), sampling time offset (STO), and IQTM. Since the single-carrier frequency domain equalization (SC-FDE) can be viewed as discrete Fourier transform (DFT) precoded OFDM, our signal model will be presented based on OFDM with a DFT size of N_{DFT}. The TX has U_T digital-to-analog conversion (DAC) branches and each branch is connected to V_T antenna elements. The RX has U_R analog-to-digital conversion (ADC) branches and each branch is connected to V_R antenna elements. The DAC (ADC) branch index is denoted by u_1 (u_2) and the antenna index connected to a DAC (ADC) branch is referred to by v_1 (v_2).

Let $\{c_{u_1,k}\}$ represent the TX IDFT output signal (after cyclic prefix (CP) insertion) for the input frequency-domain symbols $\{C_{u_1}[k]\}$. Denote the TX pulse shape filter impulse response as $g_T(t)$ and the TX sampling period at the output of IDFT as T_s. The OFDM modulated and pulse shape filtered signal at the DAC branch u_1 without IQTM is given by

$$s_{u_1}(t) = \sum_k c_{u_1,k} g_T(t - kT_s). \tag{1}$$

When there is IQTM at TX, such time mismatch can be modeled by introducing a time delay τ_{tx,u_1} to the imaginary part of $s_{u_1}(t)$ with respect to the real part of $s_{u_1}(t)$ (or the reverse order), where τ_{tx} can take either a positive or negative value. With the IQTM, the signal at the output of the DAC branch u_1 becomes

$$\breve{s}_{u_1}(t) = \Re\{s_{u_1}(t)\} + j\Im\{s_{u_1}(t - \tau_{\mathrm{tx},u_1})\} \tag{2}$$

where $\Re\{\cdot\}$ and $\Im\{\cdot\}$ denote the real part and imaginary part respectively. The effects of TX IQI and PN are modeled by

$$x_{u_1,v_1}(t) = \left[\mu_{T,u_1,v_1}\breve{s}_{u_1}(t) + \nu_{T,u_1,v_1}\breve{s}^*_{u_1}(t)\right] e^{j\phi_{T,u_1}(t)} \tag{3}$$

978-1-5090-2482-7/16/$31.00 ©2016 IEEE

where μ_{T,u_1,v_1} and ν_{T,u_1,v_1} are TX IQI coefficients, $e^{j\phi_{T,u_1}(t)}$ is TX PN (which also absorbs TX CFO), and the superscript * is the conjugate operation. Next, the received signal at antenna v_2 in ADC branch u_2 is given by

$$r_{u_2,v_2}(t) = \sum_{u_1=1}^{U_T}\sum_{v_1=1}^{V_T}\sum_{l=1}^{L} x_{u_1,v_1}(t-\tau_l)e^{j\theta_{T,u_1,v_1}} h_{u_1,v_1}^{u_2,v_2}(t,l) + w_{u_2,v_2}(t) \quad (4)$$

where we assume that each multipath channel has L paths, $h_{u_1,v_1}^{u_2,v_2}(t,l)$ is the lth tap channel coefficient at time t between antenna element v_1 in TX DAC branch u_1 and antenna element v_2 in RX ADC branch u_2, $e^{j\theta_{T,u_1,v_1}}$ is the TX analog beamforming coefficient, and $w_{u_2,v_2}(t)$ is an additive white Gaussian noise process. Then, after analog beamforming at RX, the signal at the ADC branch u_2 is given by

$$r_{u_2}(t) = \sum_{v_2=1}^{V_R} e^{j\theta_{R,u_2,v_2}} r_{u_2,v_2}(t) \quad (5)$$

where $e^{j\theta_{R,u_2,v_2}}$ is the RX analog beamforming coefficient.

Let μ_{R,u_2} and ν_{R,u_2} denote the RX IQI coefficients, α_{u_2} be the RX CFO, $g_R(t)$ stand for the impulse response of the RX filter, and $e^{-j\phi_{R,u_2}(t)}$ represent the RX PN. After experiencing PN, CFO and IQI, the signal becomes

$$\begin{aligned}\tilde{y}_{u_2}(t) =& \mu_{R,u_2}\left(r_{u_2}(t)e^{-j\phi_{R,u_2}(t)}e^{-j2\pi\alpha_{u_2}t}\right) \\ &+ \nu_{R,u_2}\left(r_{u_2}(t)e^{-j\phi_{R,u_2}(t)}e^{-j2\pi\alpha_{u_2}t}\right)^*. \end{aligned} \quad (6)$$

After passing through the receive filter, the output signal is

$$y_{u_2}(t) = \tilde{y}_{u_2}(t) * g_R(t) \quad (7)$$

where $*$ denotes the convolution. Define the following:

$$\bar{r}_{u_2}(t) \triangleq r_{u_2}(t)e^{-j\phi_{R,u_2}(t)} \quad (8)$$

$$\tilde{g}_R(t) \triangleq e^{j2\pi\alpha_{u_2}t} g_R(t). \quad (9)$$

$$\begin{aligned}\tilde{r}_{u_2}(t) &\triangleq e^{-j2\pi\alpha_{u_2}t}\left\{\bar{r}_{u_2}(t) * \tilde{g}_R(t)\right\} \\ &= e^{-j2\pi\alpha_{u_2}t}\left\{(r_{u_2}(t)e^{-j\phi_{R,u_2}(t)}) * \tilde{g}_R(t)\right\}. \end{aligned} \quad (10)$$

Then, we can express (7) as

$$y_{u_2}(t) = \mu_{R,u_2}\tilde{r}_{u_2}(t) + \nu_{R,u_2}\tilde{r}^*_{u_2}(t) \quad (11)$$

When there is a RX IQTM, such time mismatch can be modeled by introducing a time delay τ_{rx,u_2} to the imaginary part of $y_{u_2}(t)$ with respect to the real part of $y_{u_2}(t)$. Then, the corresponding receive filter output signal is

$$\breve{y}_{u_2}(t) = \Re\{y_{u_2}(t)\} + j\Im\{y_{u_2}(t-\tau_{\mathrm{rx},u_2})\}. \quad (12)$$

If there is a SFO between the sampling frequencies of TX IDFT and RX DFT, then the RX DFT sampling period T_s' would be different from the TX IDFT sampling period T_s. Furthermore, the RX filter output sampling time instant could deviate from the optimal sampling instant, resulting a sampling time offset t_0. Then, the sampled version of (12) is given by $\breve{y}_{u_2}[k] = \breve{y}_{u_2}(kT_s' + t_0)$. After the CP removal, applying DFT to the N_{DFT} samples $\{\breve{y}_{u_2}[k]\}$ of an OFDM symbol yields the received signals $\{\breve{Y}_{u_2}[n]\}$ on the N_{DFT} subcarriers where n is the subcarrier index.

Suppose the system uses N ($< N_{\mathrm{DFT}}$) subcarriers with subcarrier indexes $\{k_i : i = 1, \cdots, N\}$ where k_i and k_{N+1-i} are a mirror tone pair, i.e., $k_i = -k_{N+1-i}$ modulo N_{DFT}. Define the frequency-domain received signal vector as $\breve{\mathbf{Y}}_{u_2} = [\breve{Y}_{u_2}[k_1], \cdots, \breve{Y}_{u_2}[k_N]]^T$ and the frequency-domain transmit signal vector from the DAC branch u_1 as $\mathbf{C}_{u_1} = [C_{u_1}[k_1], \cdots, C_{u_1}[k_N]]^T$. Next, for a compact presentation, for a vector $\mathbf{X}$, let $[\mathbf{X}]_{\mathrm{RI}}$ represent $[\Re\{\mathbf{X}^T\}, \Im\{\mathbf{X}^T\}]^T$ where the superscript T is the transpose operator. Then, after some manipulation (details are omitted due to the space limitation), we obtain an approximate frequency-domain signal model in the matrix form as

$$[\breve{\mathbf{Y}}_{u_2}]_{\mathrm{RI}} \approx \sum_{u_1=1}^{U_T} \mathbf{\Lambda}_{\mathrm{rx},u_2}\mathbf{Q}_{u_2u_1}\mathbf{\Lambda}_{\mathrm{tx},u_1}[\mathbf{C}_{u_1}]_{\mathrm{RI}} + [\breve{\eta}_{u_2}]_{\mathrm{RI}} \quad (13)$$

where $\mathbf{\Lambda}_{\mathrm{tx},u_1}$ and $\mathbf{\Lambda}_{\mathrm{rx},u_2}$ are the matrices representing the TX IQTM effect and the RX IQTM effect and they are given by (14) and (15) (see at the top of next page) with $\mathbf{J} = \mathrm{fliplr}(\mathbf{I})$ where fliplr is the MATLAB function which flips the matrix (or row vector) from left to right, and

$$\mathbf{\Lambda}_{\mathrm{D}}(\tau) = \mathrm{diag}\left\{\frac{1+e^{\frac{-j2\pi k_1\tau}{N_{\mathrm{DFT}}T_s'}}}{2}, \cdots, \frac{1+e^{\frac{-j2\pi k_N\tau}{N_{\mathrm{DFT}}T_s'}}}{2}\right\}, \quad (16)$$

$$\mathbf{\Lambda}_{\mathrm{M}}(\tau) = \mathrm{diag}\left\{\frac{1-e^{\frac{-j2\pi k_1\tau}{N_{\mathrm{DFT}}T_s'}}}{2}, \cdots, \frac{1-e^{\frac{-j2\pi k_N\tau}{N_{\mathrm{DFT}}T_s'}}}{2}\right\}. \quad (17)$$

In (13), $\mathbf{Q}_{u_2u_1}$ is the matrix representing the combined effects of the channel and all considered RF distortions except IQTM, and $\breve{\eta}_{u_2}$ is the corresponding frequency-domain complex noise vector. The equation (13) shows the decoupled operations of IQTM and other RF distortions. When $\tau_{\mathrm{tx},u_1} = \tau_{\mathrm{rx},u_2} = 0$, the IQTM matrices $\mathbf{\Lambda}_{\mathrm{tx},u_1}$ and $\mathbf{\Lambda}_{\mathrm{rx},u_2}$ reduce to an identity matrix. In all of the above equations, the OFDM symbol index is omitted for simplicity. We will include the OFDM symbol index in later parts of the paper when needed.

Note that we use the time-domain signal models to generate signals in our simulation while we apply the frequency-domain signal model in our pilot designs, estimator development, and IQTM compensation.

III. Pilot Designs for IQTMs

A. Joint TX and RX IQTMs or TX-only IQTM

Suppose $\{\tilde{\tau}_{\mathrm{rx},u_2}^{(i)} : i = 1, 2, \cdots, n_{\tau,u_2}\}$ and $\{\tilde{\tau}_{\mathrm{tx},u_1}^{(m)} : m = 1, 2, \cdots, n_{\tau,u_1}\}$ represent the sets of the trial candidate values for the RX IQTM and the TX IQTM, respectively. Let $\mathbf{C}_{u_1}^{(m)}$ be the $N \times 1$ pilot vector to be used for $\tilde{\tau}_{\mathrm{tx},u_1}^{(m)}$ and its subcarrier indexes are mirror pairs.

First, we define an initial non-zero pilot tone index set $J_{\mathrm{ini}} = \{J_{\mathrm{ini}}^{\mathrm{L}}, J_{\mathrm{ini}}^{\mathrm{R}}\}$ where $J_{\mathrm{ini}}^{\mathrm{L}}$ and $J_{\mathrm{ini}}^{\mathrm{R}}$ represent the index sets of the initial non-zero pilot tones at the left side and the right side of the DC tone, respectively. Suppose that

$$\mathbf{\Lambda}_{\mathrm{tx},u_1} = \begin{bmatrix} (\Re[\mathbf{\Lambda}_{\mathrm{D}}(\tau_{\mathrm{tx},u_1})] + \Re[\mathbf{\Lambda}_{\mathrm{M}}(\tau_{\mathrm{tx},u_1})]\mathbf{J}), & (-\Im[\mathbf{\Lambda}_{\mathrm{D}}(\tau_{\mathrm{tx},u_1})] + \Im[\mathbf{\Lambda}_{\mathrm{M}}(\tau_{\mathrm{tx},u_1})]\mathbf{J}) \\ (\Im[\mathbf{\Lambda}_{\mathrm{D}}(\tau_{\mathrm{tx},u_1})] + \Im[\mathbf{\Lambda}_{\mathrm{M}}(\tau_{\mathrm{tx},u_1})]\mathbf{J}), & (\Re[\mathbf{\Lambda}_{\mathrm{D}}(\tau_{\mathrm{tx},u_1})] - \Re[\mathbf{\Lambda}_{\mathrm{M}}(\tau_{\mathrm{tx},u_1})]\mathbf{J}) \end{bmatrix}, \tag{14}$$

$$\mathbf{\Lambda}_{\mathrm{rx},u_2} = \begin{bmatrix} (\Re[\mathbf{\Lambda}_{\mathrm{D}}(\tau_{\mathrm{rx},u_2})] + \Re[\mathbf{\Lambda}_{\mathrm{M}}(\tau_{\mathrm{rx},u_2})]\mathbf{J}), & (-\Im[\mathbf{\Lambda}_{\mathrm{D}}(\tau_{\mathrm{rx},u_2})] + \Im[\mathbf{\Lambda}_{\mathrm{M}}(\tau_{\mathrm{rx},u_2})]\mathbf{J}) \\ (\Im[\mathbf{\Lambda}_{\mathrm{D}}(\tau_{\mathrm{rx},u_2})] + \Im[\mathbf{\Lambda}_{\mathrm{M}}(\tau_{\mathrm{rx},u_2})]\mathbf{J}), & (\Re[\mathbf{\Lambda}_{\mathrm{D}}(\tau_{\mathrm{rx},u_2})] - \Re[\mathbf{\Lambda}_{\mathrm{M}}(\tau_{\mathrm{rx},u_2})]\mathbf{J}) \end{bmatrix}, \tag{15}$$

the indexes of the used subcarriers are $-N_L, \cdots, N_R$. Note that other RF distortions such as PN and IQI introduce inter-subcarrier interference (ICI) and mirror tone interference (MTI) in frequency-domain. Assume that the one-side significant ICI spread is κ subcarriers and one-side significant MTI spread is ι subcarriers[1]. We design J_{ini} such that the individual ICI and MTI spreads of the non-zero pilot tones are decoupled. To achieve this condition, the spacing of non-zero pilot tones must be at least $(2\kappa + 2\iota + 2)$ tones at each side of the DC tone, and the non-zero pilot tones at the left side and at the right side are offset by $(\kappa + \iota + 1)$ tones. Mathematically, we design J_{ini} as

$$J_{\mathrm{ini}}^{\mathrm{R}} = \kappa + 1 : (2\kappa + 2\iota + 2) : N_R \tag{18}$$

$$J_{\mathrm{ini}}^{\mathrm{L}} = \mathrm{fliplr}(-J_{\mathrm{ini}}^{\mathrm{R}}) - \kappa - \iota - 1 \tag{19}$$

Alternatively, we can set

$$J_{\mathrm{ini}}^{\mathrm{L}} = \mathrm{fliplr}(-\kappa - 1 : (-2\kappa - 2\iota - 2) : -N_L) \tag{20}$$

$$J_{\mathrm{ini}}^{\mathrm{R}} = \mathrm{fliplr}(-J_{\mathrm{ini}}^{\mathrm{L}}) + \kappa + \iota + 1 \tag{21}$$

which satisfy the required pilot condition.

We consider a single TX DAC branch first (while keeping DAC branch index u_1 for a clear connection to the case with multiple DACs), and later we will extend the pilot design to multiple DAC branches. As we will develop different pilot sets for different trial candidate values $\{\tilde{\tau}_{\mathrm{tx},u_1}^{(m)}\}$, let J_m^{L} and J_m^{R} represent the initial non-zero pilot tone index sets at the left and right side of the DC tone for $\tilde{\tau}_{\mathrm{tx},u_1}^{(m)}$. Furthermore, let $[J_{\mathrm{ini}}^{\mathrm{L}}]_k$ and $[J_{\mathrm{ini}}^{\mathrm{R}}]_k$ stand for the kth elements of $J_{\mathrm{ini}}^{\mathrm{L}}$ and $J_{\mathrm{ini}}^{\mathrm{R}}$, respectively. Then, we design the initial pilot tone index set $J_m = \{J_m^{\mathrm{L}}, J_m^{\mathrm{R}}\}$ for $\tilde{\tau}_{\mathrm{tx},u_1}^{(m)}$ as

$$J_m^{\mathrm{L}} = \{[J_{\mathrm{ini}}^{\mathrm{L}}]_m, [J_{\mathrm{ini}}^{\mathrm{L}}]_{m+n_{\tau,u_1}}, [J_{\mathrm{ini}}^{\mathrm{L}}]_{m+2n_{\tau,u_1}}, \cdots\} \tag{22}$$

$$J_m^{\mathrm{R}} = \{[J_{\mathrm{ini}}^{\mathrm{R}}]_m, [J_{\mathrm{ini}}^{\mathrm{R}}]_{m+n_{\tau,u_1}}, [J_{\mathrm{ini}}^{\mathrm{R}}]_{m+2n_{\tau,u_1}}, \cdots\}. \tag{23}$$

Next, we design the pilot vector $\mathbf{C}_{u_1}^{(m)}$ for $\tilde{\tau}_{\mathrm{tx},u_1}^{(m)}$. Let $\boldsymbol{p}_m$ denote a $|J_m| \times 1$ vector containing constant amplitude low peak-to-average power ratio (PAPR) sequence for $\tilde{\tau}_{\mathrm{tx},u_1}^{(m)}$, and $\mathbf{\Pi}_m$ represent the $N \times |J_m|$ matrix which assigns $\boldsymbol{p}_m$ to the subcarrier indexes defined by J_m. Let the TX IQTM matrix $\mathbf{\Lambda}_{\mathrm{tx},u_1}$ for $\tau_{\mathrm{tx},u_1} = \tilde{\tau}_{\mathrm{tx},u_1}^{(m)}$ be denoted by $\mathbf{\Lambda}_{\mathrm{tx},u_1}(\tilde{\tau}_{\mathrm{tx},u_1}^{(m)})$. From (13), we observe that we can design $\mathbf{C}_{u_1}^{(m)}$ so that the effect of the TX IQTM for $\tau_{\mathrm{tx},u_1} = \tilde{\tau}_{\mathrm{tx},u_1}^{(m)}$ is pre-compensated. This design is given by

$$[\mathbf{C}_{u_1}^{(m)}]_{\mathrm{RI}} = \mathbf{\Lambda}_{\mathrm{tx},u_1}(-\tilde{\tau}_{\mathrm{tx},u_1}^{(m)})\ [\mathbf{\Pi}_m \boldsymbol{p}_m]_{\mathrm{RI}}. \tag{24}$$

[1]See [16] for how to set the values of κ and ι.

Note that $\mathbf{C}_{u_1}^{(m)}$ has non-zero elements only at the subcarriers defined by J_m for $\tilde{\tau}_{\mathrm{tx},u_1}^{(m)} = 0$ and by $\{\pm J_m\}$ for $\tilde{\tau}_{\mathrm{tx},u_1}^{(m)} \neq 0$. The TX pilot vector is

$$\mathbf{C}_{u_1} = \sum_{m=1}^{n_{\tau,u_1}} \mathbf{C}_{u_1}^{(m)}. \tag{25}$$

If multiple preamble symbols with the symbol index set $\mathcal{T}$ are used, we denote the tone index sets by including the symbol index $t \in \mathcal{T}$. In this case, we have

$$J_{\mathrm{ini},t}^{\mathrm{L}} = J_{\mathrm{ini}}^{\mathrm{L}},\ t \in \mathcal{T} \tag{26}$$

$$J_{\mathrm{ini},t}^{\mathrm{R}} = J_{\mathrm{ini}}^{\mathrm{R}},\ t \in \mathcal{T} \tag{27}$$

$$J_{m,t}^{\mathrm{R}} = \{[J_{\mathrm{ini}}^{\mathrm{R}}]_{\beta_{t,m}+m}, [J_{\mathrm{ini}}^{\mathrm{R}}]_{\beta_{t,m}+m+n_{\tau,u_1}}, \cdots\},\ t \in \mathcal{T} \tag{28}$$

$$J_{m,t}^{\mathrm{L}} = \{[J_{\mathrm{ini}}^{\mathrm{L}}]_{\beta_{t,m}+m}, [J_{\mathrm{ini}}^{\mathrm{L}}]_{\beta_{t,m}+m+n_{\tau,u_1}}, \cdots\},\ t \in \mathcal{T} \tag{29}$$

where $\{\beta_{t,m}\}$ are chosen such that the non-zero pilot tone indexes of a trial candidate transmit IQTM collected from all the preamble symbols cover the subcarrier index range approximately evenly, and for $t \in \mathcal{T}$,

$$\{J_{m_1,t}^{\mathrm{R}}, J_{m_1,t}^{\mathrm{L}}\} \cap \{J_{m_2,t}^{\mathrm{R}}, J_{m_2,t}^{\mathrm{L}}\} = \emptyset, \quad m_1 \neq m_2. \tag{30}$$

Also note that $\{J_{m,t_1}^{\mathrm{R}}, J_{m,t_1}^{\mathrm{L}}\} \cap \{J_{m,t_2}^{\mathrm{R}}, J_{m,t_2}^{\mathrm{L}}\} = \emptyset,\ t_1 \neq t_2$.

For $\tilde{\tau}_{\mathrm{tx},u_1}^{(m)}$ at symbol $t \in \mathcal{T}$, denote the constant amplitude low-PAPR sequence vector by $\boldsymbol{p}_{m,t}$, the subcarrier assignment matrix by $\mathbf{\Pi}_{m,t}$, and the corresponding pilot vector by $\mathbf{C}_{u_1,t}^{(m)}$. Then, $\mathbf{C}_{u_1,t}^{(m)}$ is designed as

$$[\mathbf{C}_{u_1,t}^{(m)}]_{\mathrm{RI}} = \mathbf{\Lambda}_{\mathrm{tx},u_1}(-\tilde{\tau}_{\mathrm{tx},u_1}^{(m)})\ [\mathbf{\Pi}_{m,t} \boldsymbol{p}_{m,t}]_{\mathrm{RI}},\ t \in \mathcal{T}. \tag{31}$$

The TX pilot vector at preamble symbol t is

$$\mathbf{C}_{u_1,t} = \sum_{m=1}^{n_{\tau,u_1}} \mathbf{C}_{u_1,t}^{(m)},\ t \in \mathcal{T}. \tag{32}$$

B. RX-only IQTM

For the scenario with RX-only IQTM, the pilot design is simply given by the non-zero pilot tone index set J_{ini} as defined in (18) and (19) or (20) and (21), and the constant amplitude low-PAPR sequence transmitted on J_{ini}. All of the RX IQTM estimate candidates use the same received pilots located at $\pm J_{\mathrm{ini}}$. In this case, one preamble symbol is typically sufficient if $|J_{\mathrm{ini}}|$ is reasonably large to yield a reliable variance metric. If multiple preamble symbols are used, the same preamble can be repeated.

IV. Estimation and Compensation of IQTMs

A. Estimation Metric

For a TX non-zero pilot tone at index n and a TX null tone at index $-n$, define $\xi_n \triangleq \frac{\breve{Y}_{u_2}[-n]}{\breve{Y}^*_{u_2}[n]}$. After some simplification (details are omitted due to the space limitation) of (13), we observe that ξ_n is approximately constant ($\approx \frac{\nu_{R,u_2}}{\mu^*_{R,u_2}}$) across non-zero pilot tone index n if there is no IQTM, but ξ_n varies across n if there are IQTM. Thus, we use the variance of ξ_n, denoted σ^2_ξ, as the metric for estimating the IQTMs.

B. Joint Estimation of TX and RX IQTMs

Suppose that the system has both TX and RX IQTMs and it uses the corresponding pilots (preambles) described in the previous section. First, we apply compensation of RX IQTM based on a candidate $\tilde{\tau}^{(i)}_{\mathrm{rx},u_2}$ on the received frequency-domain vector at OFDM symbol $t \in \mathcal{T}$ as

$$[(\breve{\mathbf{Y}}^{(i)}_{u_2,t})]_{\mathrm{RI}} = \mathbf{\Lambda}_{\mathrm{rx},u_2}(-\tilde{\tau}^{(i)}_{\mathrm{rx},u_2})\ [\breve{\mathbf{Y}}_{u_2,t}]_{\mathrm{RI}} \tag{33}$$

where $\mathbf{\Lambda}_{\mathrm{rx},u_2}(-\tilde{\tau}^{(i)}_{\mathrm{rx},u_2})$ is given by (15) with τ_{rx,u_2} replaced by $-\tilde{\tau}^{(i)}_{\mathrm{rx},u_2}$. Next, for a candidate IQTM pair $(\tilde{\tau}^{(m)}_{\mathrm{tx},u_1}, \tilde{\tau}^{(i)}_{\mathrm{rx},u_2})$ and $n \in J_{m,t}$ with $t \in \mathcal{T}$, we define and compute $\xi^{(m,i)}_{n,t}$ as

$$\xi^{(m,i)}_{n,t} = \frac{\breve{Y}^{(i)}_{u_2,t}[-n]}{(\breve{Y}^{(i)}_{u_2,t}[n])^*} \tag{34}$$

and the estimation metric value as

$$\sigma^2_\xi(\tilde{\tau}^{(m)}_{\mathrm{tx},u_1}, \tilde{\tau}^{(i)}_{\mathrm{rx},u_2}) = \left(\frac{1}{\sum_{t\in\mathcal{T}}|J_{m,t}|}\sum_{t\in\mathcal{T}}\sum_{n\in J_{m,t}}|\xi^{(m,i)}_{n,t}|^2\right) - \left|\frac{1}{\sum_{t\in\mathcal{T}}|J_{m,t}|}\sum_{t\in\mathcal{T}}\sum_{n\in J_{m,t}}\xi^{(m,i)}_{n,t}\right|^2. \tag{35}$$

Among the candidate IQTM pairs $\{(\tilde{\tau}^{(m)}_{\mathrm{tx},u_1}, \tilde{\tau}^{(i)}_{\mathrm{rx},u_2})\}$, the estimator chooses the one with the smallest metric value as

$$(\hat{\tau}_{\mathrm{tx},u_1}, \hat{\tau}_{\mathrm{rx},u_2}) = \arg_{\{(\tilde{\tau}^{(m)}_{\mathrm{tx},u_1}, \tilde{\tau}^{(i)}_{\mathrm{rx},u_2})\}} \min\{\sigma^2_\xi(\tilde{\tau}^{(m)}_{\mathrm{tx},u_1}, \tilde{\tau}^{(i)}_{\mathrm{rx},u_2})\}. \tag{36}$$

C. Estimation of TX-only IQTM

Consider the scenario with TX-only IQTM and the corresponding pilots as described in the previous section. Then, no RX-side compensation is needed and we define and compute

$$\xi^{(m)}_{n,t} = \frac{\breve{Y}_{u_2,t}[-n]}{(\breve{Y}_{u_2,t}[n])^*}, \quad n \in J_{m,t},\ t \in \mathcal{T}, \tag{37}$$

$$\sigma^2_\xi(\tilde{\tau}^{(m)}_{\mathrm{tx},u_1}) = \left(\frac{1}{\sum_{t\in\mathcal{T}}|J_{m,t}|}\sum_{t\in\mathcal{T}}\sum_{n\in J_{m,t}}|\xi^{(m)}_{n,t}|^2\right) - \left|\frac{1}{\sum_{t\in\mathcal{T}}|J_{m,t}|}\sum_{t\in\mathcal{T}}\sum_{n\in J_{m,t}}\xi^{(m)}_{n,t}\right|^2. \tag{38}$$

Then, the corresponding TX IQTM estimator is given by

$$\hat{\tau}_{\mathrm{tx},u_1} = \arg_{\{\tilde{\tau}^{(m)}_{\mathrm{tx},u_1}\}} \min\{\sigma^2_\xi(\tilde{\tau}^{(m)}_{\mathrm{tx},u_1})\}. \tag{39}$$

D. Estimation of RX-only IQTM

Suppose IQTM only exists at RX and the corresponding pilots described in the previous section are used. First, we apply compensation of RX IQTM based on a candidate $\tilde{\tau}^{(i)}_{\mathrm{rx},u_2}$ as in (33) to the frequency-domain received vector at preamble symbol $t \in \mathcal{T}$. Then, we define and compute

$$\xi^{(i)}_{n,t} = \frac{\breve{Y}^{(i)}_{u_2,t}[-n]}{(\breve{Y}^{(i)}_{u_2,t}[n])^*}, \quad n \in J_{\mathrm{ini}},\ t \in \mathcal{T}, \tag{40}$$

$$\sigma^2_\xi(\tilde{\tau}^{(i)}_{\mathrm{rx},u_2}) = \left(\frac{1}{|\mathcal{T}||J_{\mathrm{ini}}|}\sum_{t\in\mathcal{T}}\sum_{n\in J_{\mathrm{ini}}}|\xi^{(i)}_{n,t}|^2\right) - \left|\frac{1}{|\mathcal{T}||J_{\mathrm{ini}}|}\sum_{t\in\mathcal{T}}\sum_{n\in J_{\mathrm{ini}}}\xi^{(i)}_{n,t}\right|^2. \tag{41}$$

The corresponding RX IQTM estimator is given by

$$\hat{\tau}_{\mathrm{rx},u_2} = \arg_{\{\tilde{\tau}^{(i)}_{\mathrm{rx},u_2}\}} \min\{\sigma^2_\xi(\tilde{\tau}^{(i)}_{\mathrm{rx},u_2})\}. \tag{42}$$

E. IQTM Compensation

For a transceiver with stored IQTM estimates of $\{\hat{\tau}_{\mathrm{tx},u_1}\}$ and $\{\hat{\tau}_{\mathrm{rx},u_2}\}$, the TX IQTM compensation is performed on the frequency-domain data vector as

$$[\tilde{\mathbf{C}}_{u_1}]_{\mathrm{RI}} = \mathbf{\Lambda}_{\mathrm{tx},u_1}(-\hat{\tau}_{\mathrm{tx},u_1})\ [\mathbf{C}_{u_1}]_{\mathrm{RI}} \tag{43}$$

where $\tilde{\mathbf{C}}_{u_1}$ becomes IDFT inputs for OFDM signal generation. The RX IQTM compensation is performed on the DFT output frequency-domain vector at RX as

$$[(\tilde{\mathbf{Y}}_{u_2})]_{\mathrm{RI}} = \mathbf{\Lambda}_{\mathrm{rx},u_2}(-\hat{\tau}_{\mathrm{rx},u_2})\ [\breve{\mathbf{Y}}_{u_2}]_{\mathrm{RI}} \tag{44}$$

where $\tilde{\mathbf{Y}}_{u_2}$ is input to the modulation slicer or data detector. In the above, we presented baseband DSP-based compensation for IQTM. If the transceiver has multi-phase filters or DAC/ADC with adjustable sampling instants for introducing different delays at the TX and RX chains, IQTM compensation can also be implemented by such hardware-based mechanism.

V. Performance Evaluation

A. System Setting

We consider an OFDM system with 64 antennas at BS and 4 antennas at UE. The subcarrier spacing is 1.44 MHz and the carrier frequency is 73 GHz. The bandwidth is 250 MHz, the DFT size is 256, and the number of used subcarriers is 173. The channel model is based on the 3GPP LTE channel model with two clusters where each cluster has 20 sub-paths, the second clusters delay is about 80 ns and its power is -9 dB with reference to the first cluster. Analog beamforming is applied based on the mean arrival angle of the sub-paths of the first cluster. We consider a single data stream with 16-QAM. The PN power spectral densities (PSD) at TX and RX are independently modeled as $\mathrm{PSD}(f) = \mathrm{PSD}(0)[1 + (\frac{f}{f_z})^2]/[1 + (\frac{f}{f_p})^2]$ where PSD(0) = -60 dBc/Hz, PSD(100k) = -75 dBc/Hz and PSD(∞) = -130 dBc/Hz. The CFOs at TX and RX sides are independent and uniformly (as a worst case scenario) distributed within the

range of ± 1 ppm, the RX SFO is set at 1 ppm and the RX STO is uniformly (as a worst case scenario) distributed within $[-T_s'/2, T_s'/2]$. IQIs are independent at TX and RX sides and they are uniformly distributed within the range defined by the maximum amplitude imbalance of 4 dB and the maximum phase imbalance of 5 degrees. The mobile speed is 10 km/h. We assume no nonlinear distortion. In the simulation, signals are generated in the time domain with 4 times oversampling of the DFT sampling frequency.

As a reference, we include the performance of the estimator in [14] which assumes that CFO is pre-compensated and there are no other RF distortions. Its estimator uses two preambles with frequency-domain symbols $\{C_1[k]\}$ and $\{C_2[k]\}$ separately and require that $\frac{C_1^*[N-k+1]}{C_1[k]} - \frac{C_2^*[N-k+1]}{C_2[k]} \neq 0$ for $k \in \mathcal{P}$ where $\mathcal{P}$ is the pilot index set. The signal is intentionally transmitted on pairs of mirror subcarriers to enable the key metric function $D[k] = \frac{\check{Y}_2[k] - C_2[k]\hat{H}[k]}{\check{Y}_2^*[N-k+1] - C_{\text{ideal}}[k]\hat{H}[N-k+1]}$ in the receive IQTM only case, where $C_{\text{ideal}}[k] = C_2[k]C_1^*[N-k+1]/C_1[k]$ and $\hat{H}[k] = \check{Y}_1[k]/C_1[k]$. The principle behind this method is that the metric value $D[k]$ is a function of $\mu_R, \nu_R, \tau_{\text{rx}}$, k, and the larger τ_{rx} is, the larger the variance of $\{D[k], k \in \mathcal{P}\}$ is. Reference [14] estimates τ_{rx} by comparing the variance of $\{D[k], k \in \mathcal{P}\}$ to heuristic thresholds.

For the case with the RX-only IQTM, we use one preamble symbol with non-zero pilot tone spacing of 6 tones at each side of the DC tone and use the candidate set $\{\tilde{\tau}_{\text{rx}}^{(i)}\} = \{-T_s', -0.75T_s', \cdots, T_s'\}$. The reference estimator uses two preamble symbols and each symbol use the same amount of pilots and the same pilot tone spacing as the proposed estimator. For the case with the TX-only IQTM, we use the candidate set $\{\tilde{\tau}_{\text{tx}}^{(i)}\} = \{-T_s, -0.75T_s, \cdots, T_s\}$. The number of preamble symbols is the same as the number of candidate points for the TX IQTM. Each preamble symbol has non-zero pilot tones with tone spacing of 6 tones at each side of the DC tone and they are assigned alternately among the IQTM candidate points as described in the pilot design section.

B. Impact of IQTM on BER

We first evaluate the impact of IQTM on system's bit error rate (BER), thus no IQTM compensation is applied here. We simply consider a preamble OFDM symbol followed by a pilot-data multiplexed OFDM symbol carrying 16-QAM symbols and pilot tones. The preamble and pilots are for estimating the channel and RF distortions (other than IQTM). These preamble and pilot designs, their corresponding estimators, ICI and MTI compensation and data detection are according to [16]. In Fig. 1, we present the effects of IQTMs on BER at different E_b/N_0 values for systems with TX-only IQTM, RX-only IQTM, and both TX and RX IQTMs. We observe that the BER performance degrades as the IQTM increases and the BER performances for TX-only IQTM and RX-only IQTM are practically the same. The IQTMs at both TX and RX cause more BER degradation than the IQTM at one side only. If compared to the case without any IQTM, the BER performance degradation caused by the IQTM is substantial. The above BER results clearly demonstrate that a compensation scheme is needed to counter the effects of IQTM.

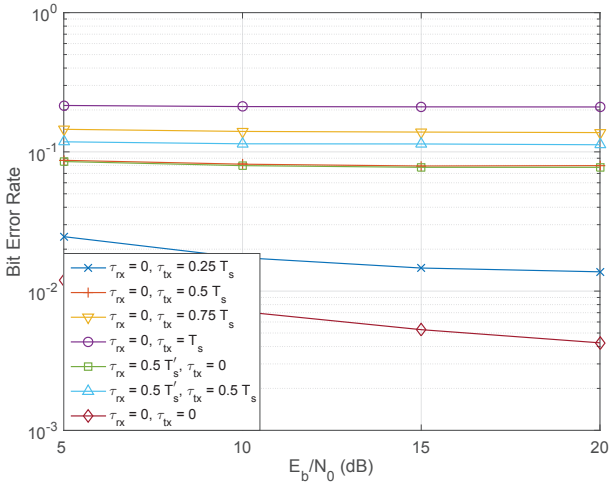

Fig. 1. The impacts of IQTMs on the system's BER performance (T_s and T_s' are the sampling periods for IDFT/DFT in OFDM modulation and demodulation, respectively).

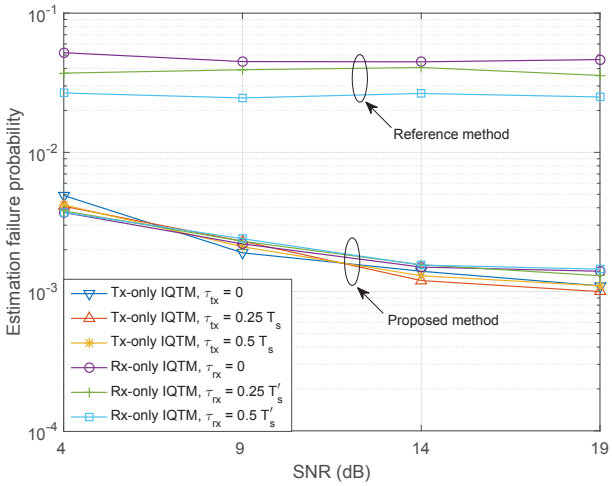

Fig. 2. Estimation failure probabilities for systems with TX-only IQTM and RX-only IQTM

C. Estimator Performance

We first evaluate TX-only IQTM case and RX-only IQTM case. Fig. 2 presents the estimation failure probability of the reference estimator for the RX-only IQTM case and the proposed IQTM estimators for the TX-only and RX-only IQTM cases. We see that the proposed RX IQTM estimator has significant advantage compared to the reference estimator. The reference estimator is developed without considering TX IQTM, so it cannot estimate TX IQTM. We also observe that the estimation failure probabilities of the proposed estimators for the TX-only and RX-only IQTM cases are similar.

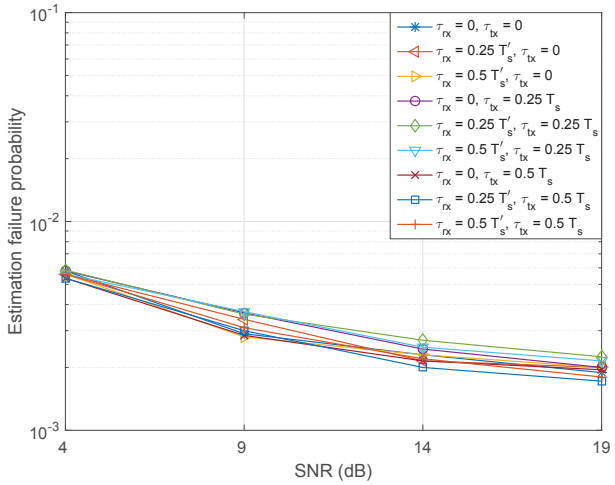

Fig. 3. TX IQTM estimation failure probability of the proposed method in systems with both TX and RX IQTMs

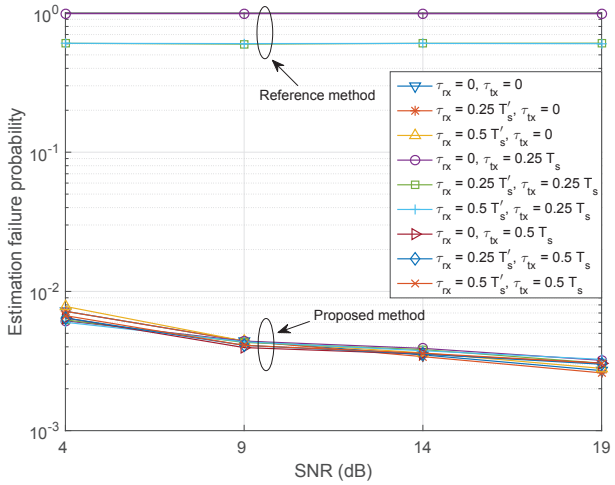

Fig. 4. RX IQTM estimation failure probability of the proposed method in systems with both TX and RX IQTMs

Next, we evaluate the estimator performance in systems with both TX and RX IQTMs. For the proposed estimator, we use the candidate set $\{\tilde{\tau}_{\text{tx}}^{(i)}\} = \{-T_s, -0.75T_s, \cdots, T_s\}$ and $\{\tilde{\tau}_{\text{rx}}^{(i)}\} = \{-T_s', -0.75T_s', \cdots, T_s'\}$. Fig. 3 and Fig. 4 show the estimation failure probability of the TX IQTM and the RX IQTM, respectively, for the proposed method under several IQTM settings. In Fig. 4, we also include the performance of the reference estimator when $\tau_{\text{tx}} = 0.25T_s$. We observe that the reference estimator fails in the presence of TX IQTM. It is expected as the reference estimator relies on heuristic thresholds which are calculated based on RX-only IQTM candidates. Next, comparing with Fig. 2, we observe that IQTMs at both the TX and RX cause larger estimation failure probability than individual IQTM cases. But the proposed method still gives good performance.

VI. Conclusions

The timing mismatches between the in-phase and quadrature paths of the transmitter and the receiver represent an important and challenging issue to overcome for millimeter-wave communication systems. We illustrated significant impact of IQTM on the system BER performance. We presented novel pilot designs as well as the IQTM estimators for TX-only IQTM, RX-only IQTM and both TX and RX IQTMs, which are applicable in OFDM and SC-FDE systems. The simulation results show that the proposed pilot designs and IQTM estimators substantially outperform the existing method in terms of estimation performance and general applicability.

References

[1] S. Rangan, T. S. Rappaport, and E. Erkip, "Millimeter-wave cellular wireless networks: Potentials and challenges," *Proc. IEEE*, vol. 102, no. 3, pp. 366–385, Mar. 2014.

[2] T. S. Rappaport, S. Sun, R. Mayzus, H. Zhao, Y. Azar, K. Wang, G. N. Wong, J. K. Schulz, M. Samimi and F. Gutierrez, "Millimeter wave mobile communications for 5G cellular: It will work!," *IEEE Access*, vol.1, pp. 335–349, May 2013.

[3] Z. Pi and F. Khan, "An introduction to millimeter-wave mobile broadband systems," *IEEE* Commun. Mag., vol.49, no. 6, pp. 101–107, Jun. 2011.

[4] A. Tarighat, R. Bagheri, and A. H. Sayed, "Compensation schemes and performance analysis of IQ imbalances in OFDM receivers," *IEEE Trans. Signal Process.*, vol. 53, no. 8, pp. 3257–3268, Aug. 2005.

[5] Y. Li, L. Fan, H. Lin, and M. Zhao, "A new method to simultaneously estimate TX/RX IQ imbalance and channel for OFDM systems," in *IEEE ICC*, June 2013, pp. 4551–4555.

[6] W. Kirkland and K. Teo, "I/Q distortion correction for OFDM direct conversion receiver," *Electron. Lett*, vol. 39, no. 1, pp. 131–133, 2003.

[7] H. Minn and D. Munoz, "Pilot designs for channel estimation of MIMO OFDM systems with frequency-dependent I/Q imbalances," *IEEE Trans. Commun.*, vol. 58, no. 8, pp. 2252–2264, Aug. 2010.

[8] L. Brötje, S. Vogeler, K.-D. Kammeyer, R. Rückriem, and S. Fechtel, "Estimation and correction of transmitter-caused I/Q imbalance in OFDM systems," in *Intl. OFDM workshop*, Sept. 2002, pp. 178–182.

[9] Y. Egashira, Y. Tanabe, and K. Sato, "A novel IQ imbalance compensation method with pilot-signals for OFDM system," in *IEEE VTC*, Sept. 2006.

[10] N. Kolomvakis, M. Matthaiou and M. Coldrey, "IQ imbalance in multiuser systems: Channel estimation and compensation," *IEEE Trans. Commun.*, vol. 64, no. 7, pp. 3039–3051, July 2016.

[11] H. Huang, W. G. Wang, and J. He, "Phase noise and frequency offset compensation in high frequency MIMO-OFDM system," in *IEEE ICC*, June 2015, pp. 1280–1285.

[12] P. Rabiei, W. Namgoong, and N. Al-Dhahir, "Reduced-complexity joint baseband compensation of phase noise and I/Q imbalance for MIMO-OFDM systems," *IEEE Trans. Wireless Commun.*, vol. 9, no. 11, pp. 3450–3460, Nov. 2010.

[13] Q. Zou, A. Tarighat, and A. H. Sayed, "Joint compensation of IQ imbalance and phase noise in OFDM wireless systems," *IEEE Trans. Commun.*, vol. 57, no. 2, pp. 404–414, Feb. 2009.

[14] W. C. Lai, Y. T. Liao and T. Y. Hsu, "A cost-effective preamble-assisted engine with skew calibrator for frequency-dependent I/Q imbalance in 4x4 MIMO-OFDM modem," *IEEE Trans. Circuits Syst. I, Reg. Papers*, vol. 60, no. 8, pp. 2199–2212, Aug. 2013.

[15] M. S. Faruk and K. Kikuchi, "Compensation for in-phase/quadrature imbalance in coherent-receiver front end for optical quadrature amplitude modulation," *IEEE Photon. J.*, vol. 5, no. 2, pp. 7800110–7800110, Apr. 2013.

[16] A. Khansefid, H. Minn, N. Al-Dhahir, H. Huang, and X. Du, "Pilot designs and compensation scheme for severe RF distortions in millimeter-wave massive MIMO systems," *IEEE Globecom MCHFB Workshop, 2016.*

Acknowledgment

This work is partially supported by Huawei Technologies Co., Ltd., China.